UDK 669.721.5:52-334.2 ISSN 1580-2949
Original scientific article/Izvirni znanstveni članek MTAEC9, 58(1)69(2024)

# EFFECT OF Zr, Zn AND Cu ADDITIONS ON ELEVATED-TEMPERATURE MECHANICAL PROPERTIES OF AS-EXTRUDED Mg-3Sn-1Ca ALLOY

# VPLIV DODATKOV Zr, Zn IN Cu NA MEHANSKE LASTNOSTI EKSTRUDIRANE ZLITINE VRSTE Mg-3Sn-1Ca PRI POVIŠANIH TEMPERATURAH

**Zheng Jia[1*], Yongzhi Yu[1], Li Fu[1], Wenyi Hu[2]**

[1]College of Mechanical Engineering, Shenyang University, Shenyang 110044, China
[2]College of Chemistry and Material Science, Longyan University, Fujian, Longyan 366300, China

*Prejem rokopisa – received: 2023-06-08; sprejem za objavo – accepted for publication: 2023-12-19*

doi:10.17222/mit.2023.904

In this study, the effects of Zr, Zn and Cu additions on the microstructure, room-temperature and high-temperature mechanical properties of an Mg-3Sn-1Ca alloy (from 25 °C to 250 °C) were studied. The results reveal that additions of Zr and Zn do not change the phase composition of the alloy, composed of CaMgSn and $Mg_2Sn$ phases. After the addition of Zn, the grains are significantly refined, the volume fraction of the second phase is increased and dispersed, and the $Mg_2Ca$ phase is precipitated. The grain refinement of Zr is better than that of Zn. After adding the Cu element, the $Mg_2Cu$ phase precipitates besides the CaMgSn phase. A comparison of mechanical properties shows that the alloy with Zr (TXK311) has the best mechanical properties at room temperature and high temperature, and the elongation of the TXK311 alloy can reach 68.3 % at 250 °C. The TXK311 alloy was comprehensively considered to find its optimum mechanical properties. The analysis shows that fine grains, a uniform phase distribution and texture play important roles in the deformation of the alloy.

Keywords: Mg-3Sn-1Ca-X alloys, indirect extrusion, CaMgSn phase, elevated-temperature mechanical properties

V članku avtorji opisujejo študijo vpliva dodatkov Zr, Zn in Cu na mikrostrukturo in mehanske lastnosti Mg zlitine vrste Mg-3Sn-1Ca v temperaturnem območju med 25 °C in 250 °C. Rezultati so pokazali, da dodatek Zr in Zn ne spremeni fazne sestave zlitine, ki v osnovi vsebuje fazi CaMgSn in $Mg_2Sn$. Po dodatku Zn je prišlo do pomembnega udrobljenja kristalnih zrn. Volumski delež druge faze se je povečal in dispergiral ter prišlo je do precipitacije faze $Mg_2Ca$. Udrobljenje kristalnih zrn zlitine je učinkovitejše pri dodatku Zr v primerjavi z dodatkom Zn. Z dodatkom Cu je prišlo poleg izločanja faze CaMgSn še do izločanja faze $Mg_2Cu$. Rezultati določitve mehanskih lastnosti so pokazali, da ima le-te najboljše zlitina z dodatkom Zr v celotnem preiskovanem temperaturnem območju. Raztezek zlitine z dodatkom Zr, označene kot TXK311, je dosegel vrednosti 68,3 % pri 250 °C. Ta zlitina ima optimalne mehanske lastnosti s fino drobno zrnato mikrostrukturo, enakomerno porazdelitev faz in njena tekstura pomembno vpliva na njeno plastično deformacijo.

Ključne besede: zlitina vrste Mg-3Sn-1Ca-X, indirektna ekstruzija, faze CaMgSn, mehanske lastnosti pri povišanih temperaturah

## 1 INTRODUCTION

As the lightest structure metal materials, magnesium alloys are widely used in the 3C electronics industry, aerospace, transportation and other fields due to their high strength and specific stiffness.[1–4] Among these alloys, Mg-Al and Mg-RE alloys, such as AZ91, AM60, Mg-Zn-RE and Mg-Gd-Y-Zr, are the most common commercial alloys.[5–7] However, it is difficult to use them at high temperatures, due to the thermal instability of the $\beta$-$Mg_{17}Al_{12}$ phase, for the Mg-Al series alloys. The Mg-Zn-RE and Mg-Gd-Y-Zr alloys with a rare-earth element are expensive and difficult to commercialize. Recently, low-price Sn has attracted much attention. Studies have shown that Sn has high solid solubility in magnesium and a significant precipitation strength. Adding 1–2 % Sn can form an $Mg_2Sn$ phase with a high melting point in magnesium and its alloys.[8] Furthermore, Mg-Sn-Ca alloy has attracted extensive attention in recent years due to its good heat resistance. After adding Ca to magnesium alloys, CaMgSn and $Mg_2Sn$ form heat-resistant phases and grains refine, improving high-temperature resistance.[9,10] Rao et al.[11] studied the hot deformation behavior of the Mg-3Sn-1Ca alloy under compression and found that CaMgSn particles caused significant back stress during hot deformation. However, the elevated-temperature mechanical behavior of the current Mg-Sn-Ca ternary alloys is still not ideal. Therefore, developing cost-effective Mg-Sn-Ca-based alloys with high strength and excellent plasticity at high temperatures is a difficult problem to solve.

It has been proven that extrusion deformation and alloying are effective methods for improving the mechanical properties of magnesium alloys.[12–14] As an inexpensive element, zinc can significantly refine grains and improve the strength and elongation of magnesium al-

*Corresponding author's e-mail:
jz140@163.com (Zheng Jia)

loys.[15–17] Wang et al.[18] found that an addition of Zn can refine the grain size. With an increase in the Zn content, the yield strength of an alloy gradually increases, while the number of $Mg_2Sn$ and $Mg_{17}Al_{12}$ particles also significantly increases, mainly due to a reduced solid solubility of Al in $\alpha$-Mg and an increased number of nucleation sites for the refined $Mg_2Sn$ phase, enhancing the synergistic effect of precipitation strengthening. Tang et al.[19] studied the effect of Zn on the microstructure and mechanical properties of an extruded Mg-5Sn alloy. The results showed that Zn can significantly refine the grain size of the alloy, and the amount of fine particles composed of $Mg_2Sn$ and MgZn phases increases significantly with an increase in the Zn content. The grain refinement can cause better comprehensive mechanical properties. Many studies have found that adding Cu to Mg-Zn alloys can refine grains and improve alloy strength.[20,21] Li et al.[22] studied the ageing behavior of an as-cast ZC62 magnesium alloy, and the research showed that Cu increases the eutectic temperature of the alloy that can be treated with solid solution at a higher temperature. In addition, more solute atoms can be dissolved into the matrix, significantly improving the ageing strengthening effect of the alloy. Zhu et al.[23] studied the effect of an addition of Cu on the mechanical properties of a ZK60 alloy, and the results showed that the elongation of the alloy can reach more than 9.0 % after the addition of Cu because the alloy grains were refined and the alloy plasticity was improved. Wang et al.[24] studied the microstructure and mechanical properties of an Mg-5Zn-3.5Sn-1Mn-0.5Ca-0.5Cu alloy in the as-cast form. Extruded and aged states were investigated, and the results showed that Cu can more effectively improve the aging hardening response of the alloy while the synergistic effect of Ca and Cu can promote aging hardening. A composite addition of Ca and Cu can significantly improve the peak hardness of the alloy after a dual aging treatment, improving the yield strength and ultimate tensile strength of the alloy.

As a common magnesium-alloy refiner, Zr is widely used without Al and Mn in magnesium alloys.[25] Xing et al.[26] found that Zr can prevent the growth of grains during solidification and promote nucleation through enrichment before crystallization, resulting in the component supercooling. They studied the form and grain refinement mechanism of Zr in Mg-Zn-Zr magnesium alloys. Xu et al.[27] studied the effect of an Mn or Zr addition on the mechanical properties of an extruded Mg-2Gd-1.2Y-0.5Zn (at.%) alloy. The results showed that the addition of Zr can more effectively refine the microstructure of a homogenized alloy and promote the dissolution of the secondary phase compared to the addition of Mn. Compared to the alloy with an Mn addition, the initial grain size of the alloy with a Zr addition is smaller, resulting in a higher DRX ratio and weaker textural strength after extrusion. High strength, medium ductility, and improved yield anisotropy were obtained in extruded alloys with the addition of Zr.

It can be seen that Zn can produce solid solution strengthening, improving the strength and plasticity of an Mg alloy, while Cu can refine the grains, change the type of the second phase in the alloy, increase the eutectic temperature of the Mg alloy and improve the ageing strengthening ability. Zr can improve the alloy strength by refining the alloy's solidification structure and grain size. However, the effects of Zr, Zn and Cu additions in Mg-3Sn-1Ca alloys have rarely been reported. In order to further improve the application field of Mg-Sn-Ca series alloys, this study has conducted research on Mg-3Sn-1Ca, Mg-3Sn-1Ca-1Zr, Mg-3Sn-1Ca-1Zn and Mg-3Sn-1Ca-1Cu alloys. The microstructures and elevated-temperature mechanical behaviors of these four alloys were systematically analyzed.

## 2 EXPERIMENTAL PART

In this experiment, Mg-3Sn-1Ca, Mg-3Sn-1Ca-1Zr, Mg-3Sn-1Ca-1Zn and Mg-3Sn-1Ca-1Cu were prepared using commercial pure Mg (99.9 *w*/%), pure Sn (99.9 *w*/%), Mg-25 %Ca and Mg-30 %Zr master alloys, pure Zn (99.9 *w*/%) and pure Cu (99.9 *w*/%). Four alloy samples were denoted as TX31, TXK311, TXZ311 and TXC311, respectively. Firstly, we put pure magnesium into preheated crucibles and then heated the crucibles to 760 °C. After the magnesium was completely melted, we removed the slag, and added Mg-30 % Zr and Cu. We stirred the melt and reduced the temperature to 710 °C. After 10 min, we continued to remove the slag, added Mg-25%Ca, Sn and Zn, respectively, stirred the mixtures for 2–3 min and poured them into $\varphi$ 65 × 240 molds under the protection of mixed gas ($CO_2$:$SF_6$ = 99:1) after a dwell time of 20 min. After cooling them to room temperature, the ingots were homogenized (400 °C/24 h). A homogenized ingot was processed into a billet with dimensions of $\varphi$ 47 × 100 mm using a lathe and then extruded backward into a bar with a diameter of 12 mm on a 300-T vertical hydraulic press. The extrusion temperature was 300 °C, the extrusion speed was 1 mm/s. Afterwards, the mechanical properties of extruded bars were tested at a rate of 1 mm/min, and the tensile temperatures were (25, 150, 200 and 250) °C, respectively.

The chemical compositions of the as-cast alloys were analyzed with an inductively coupled plasma atomic emission spectrometer (ICP-AES), and the results are shown in **Table 1**. The sampling locations of alloy microstructures are shown in **Figure 1**. A Shimadzu 700 X-ray diffraction analyzer (XRD) was used to analyze the phase (the target was Cu; the experimental voltage and current were 40 kV and 30 mA, respectively; the experimental scanning angle was 20–90°; the scanning speed was 4 °/min). The metallographic samples were sanded to 5000# and then mechanically polished with 0.5-μm diamond grinding paste. The polished samples were etched with 3g picric acid, 3 mL glacial acetic acid, 50 mL ethanol and 5 mL deionized water for 5–10 s. The

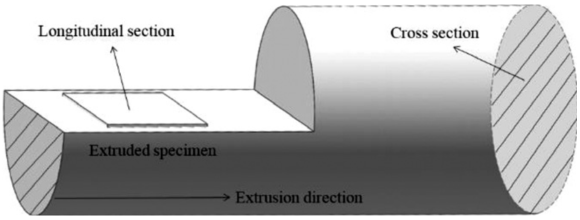


**Figure 1:** Metallographic sampling locations

morphology of the second-phase particles was observed with an S4800 scanning electron microscope (SEM) and the element composition was detected with energy dispersive spectrometer (EDS). The micro-crystallographic orientation information of the samples was obtained using the electron backscatter diffraction technique with the S4800 scanning electron microscope, and the data were analyzed with Channel 5.

**Table 1:** Actual chemical compositions of the as-cast alloys

| Alloy | Measured composition (*w*/%) | | | | | |
|---|---|---|---|---|---|---|
| | Mg | Sn | Ca | Zn | Cu | Zr |
| Mg-3Sn-Ca (TX31) | Bal. | 3.14 | 1.02 | 0 | 0 | 0 |
| Mg-3Sn-Ca-Zr (TXK311) | Bal. | 3.18 | 1.01 | 0 | 0 | 0.62 |
| Mg-3Sn-Ca-Zn (TXZ311) | Bal. | 3.12 | 1.02 | 1.09 | 0 | 0 |
| Mg-3Sn-Ca-Cu (TXC311) | Bal. | 3.22 | 1.04 | 0 | 1.07 | 0 |

## 3 RESULTS AND DISCUSSION

**Figure 2** shows optical microstructures (OMs) of the as-extruded alloys. It is evident that the average grain size of the TX31 alloy is about 3.5 μm (see **Figure 2a**); this alloy is composed of crystals with and without dynamic recrystallization. After extrusion, the TX31 alloy exhibits a bimodal structure with a mixture of coarse and fine grains, resulting in an uneven grain size. After adding Zr, the grain size of the alloy is significantly refined; there are fine equiaxed grains with an average size of about 1.8 μm. Compared to the TX31 alloy, the grains of the TXK311 alloy are refined into fine equiaxed grains, which can be explained with the peritectic reaction and component undercooling of Zr.[28] After adding Zn and Cu separately, the average grain size is 5.1 μm and 4.5 μm, respectively (see **Figures 2c** and **2d**), and the bimodal grain structure is significantly improved.

**Figure 3** shows the XRD patterns of the four alloys in the extruded state. It was found that all four alloys have diffraction peaks of the CaMgSn phase, which is consistent with the previous research reports. Regarding the Mg Sn Ca series alloys, when the mass ratio of Sn/Ca is about 3:1, almost all Ca combines with Mg and Sn to form a stable CaMgSn phase.[29] In addition, according to SEM, EDS, second phase area fraction results from **Figure 4** and **Tables 2** and **3**, it can be concluded that the addition of Zr did not generate a new second phase in the

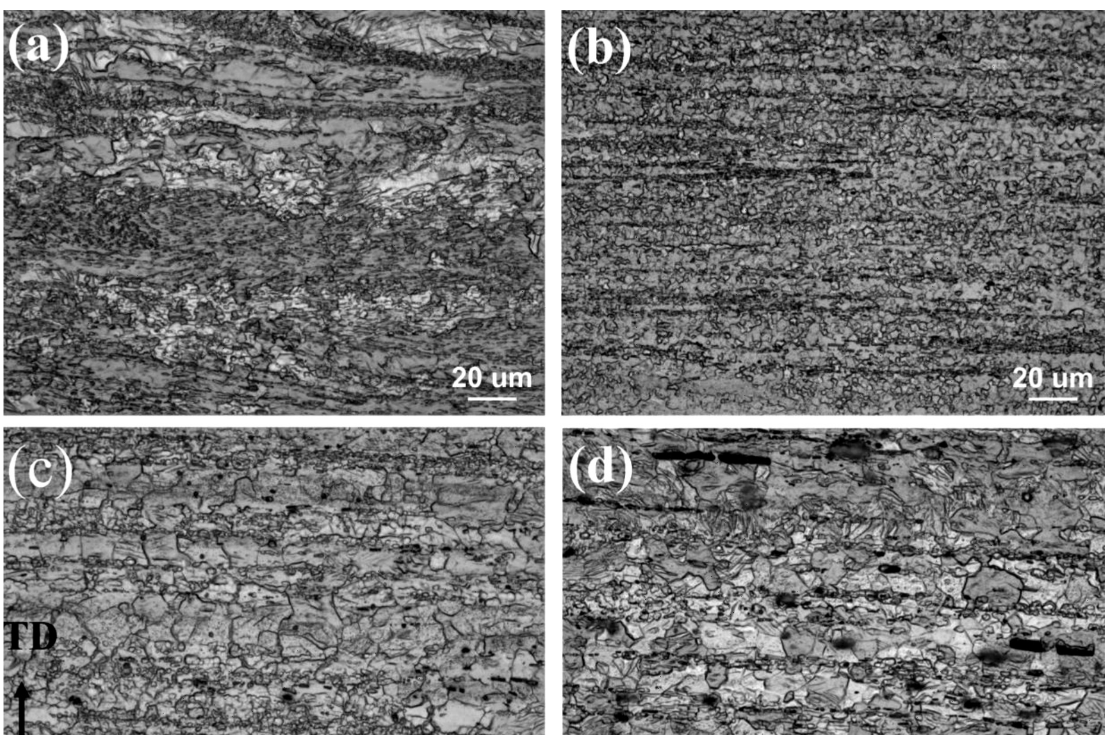


**Figure 2:** Microstructures of the as-extruded alloys: a) TX31, b) TXK31, c) TXZ311, d) TXC311

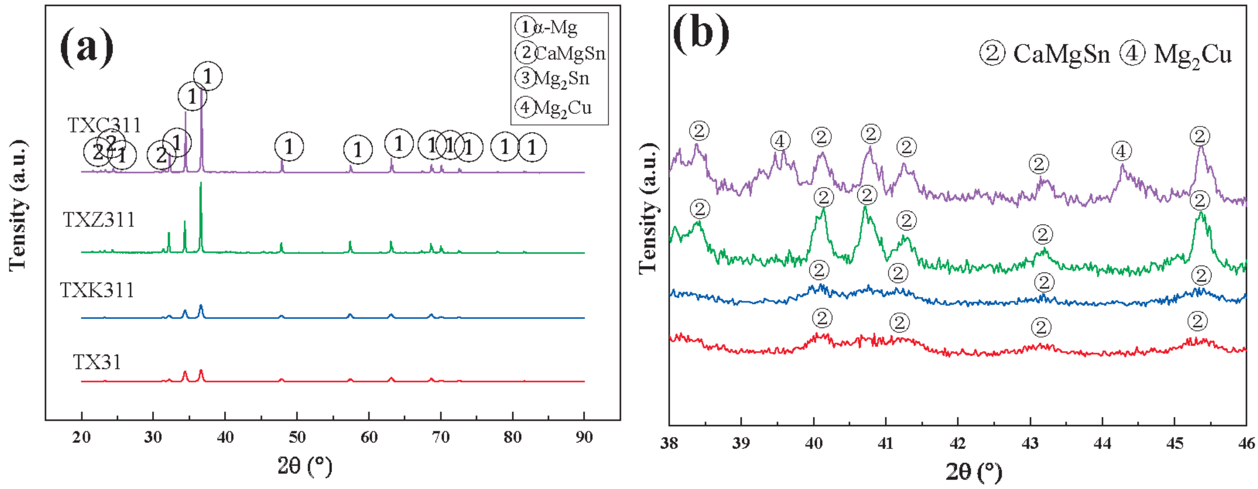


**Figure 3:** XRD patterns of the as-extruded alloys (scan angle of 20–90°)

TXK311 alloy as only the CaMgSn phase is detected; the area fraction of the second phase increased, indicating that the addition of Zr plays an important role in the grain refinement, but it cannot change the second phase in the alloy. In the TXZ311 alloy, the addition of Zn results in a coarse second-phase transition, and no intermetallic compounds containing Zn are found. In addition, the EDS results indicate that the atomic ratio of Mg/Sn at point D is greater than 2:1, indicating the presence of a small amount of $Mg_2Sn$ phase in the TXZ311 alloy, based on XRD spectroscopy. This may be due to the high solid solubility of the Zn in Mg, which is soluble in the $\alpha$-Mg matrix. According to SEM and EDS results, in addition to the massive CaMgSn phase, a spherical $Mg_2Cu$ phase was also found in the TXC311 alloy after adding Cu. Previously, Pan et al.[30] also found that an $Mg_2Cu$ phase exists in an Mg-2Sn-0.5Cu alloy, and that Cu has a significant grain refinement effect on a magnesium alloy.

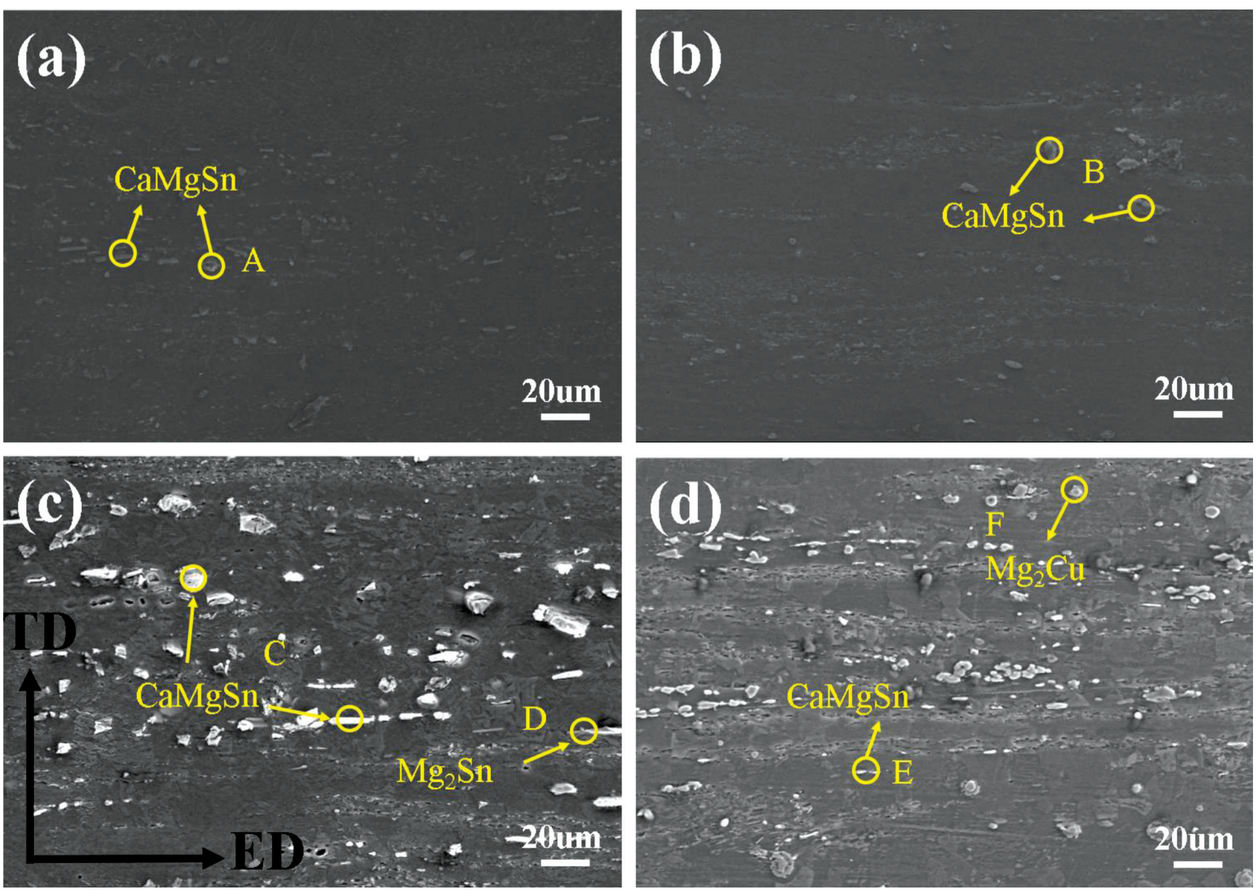


**Figure 4:** SEM images of the as-extruded alloys: a) TX31, b) TXK311, c) TXZ311, d) TXC311

**Table 2:** EDS results

| Point | Chemical composition (at.%) | | | | | Phase type |
|---|---|---|---|---|---|---|
| | Mg | Sn | Ca | Zn | Cu | |
| A | 57.2 ± 0.4 | 22.1 ± 0.6 | 19.3 ± 0.6 | – | – | MgSnCa |
| B | 86.2 ± 0.3 | 6.2 ± 0.4 | 7.7 ± 0.3 | | | MgSnCa |
| C | 66.5 ± 0.4 | 17.8 ± 0.4 | 14.6 ± 0.5 | – | – | MgSnCa |
| D | 86.6 ± 0.4 | 13.4 ± 0.5 | – | – | – | $Mg_2Sn$ |
| E | 72.9 ± 0.5 | 15.3 ± 0.4 | 11.4 ± 0.6 | – | – | MgSnCa |
| F | 72.9 ± 0.4 | – | – | – | 27.1 ± 0.6 | $Mg_2Cu$ |

**Table 3:** Area fraction and size distribution of the second phase

| Alloy | Area fraction of second phase (%) | Second-phase size distribution (μm) | | |
|---|---|---|---|---|
| | | $Mg_2Sn$ | $Mg_2Cu$ | CaMgSn |
| TX31 | 2.1 ± 0.7 | – | – | 0.6–16.8 |
| TXK311 | 3.2 ± 0.6 | – | – | 0.4–18.9 |
| TXZ311 | 5.5 ± 0.4 | 1.3–5 | – | 1.1–23.9 |
| TXC311 | 7.1 ± 0.4 | – | 3.5–8 | 1.2–24.8 |

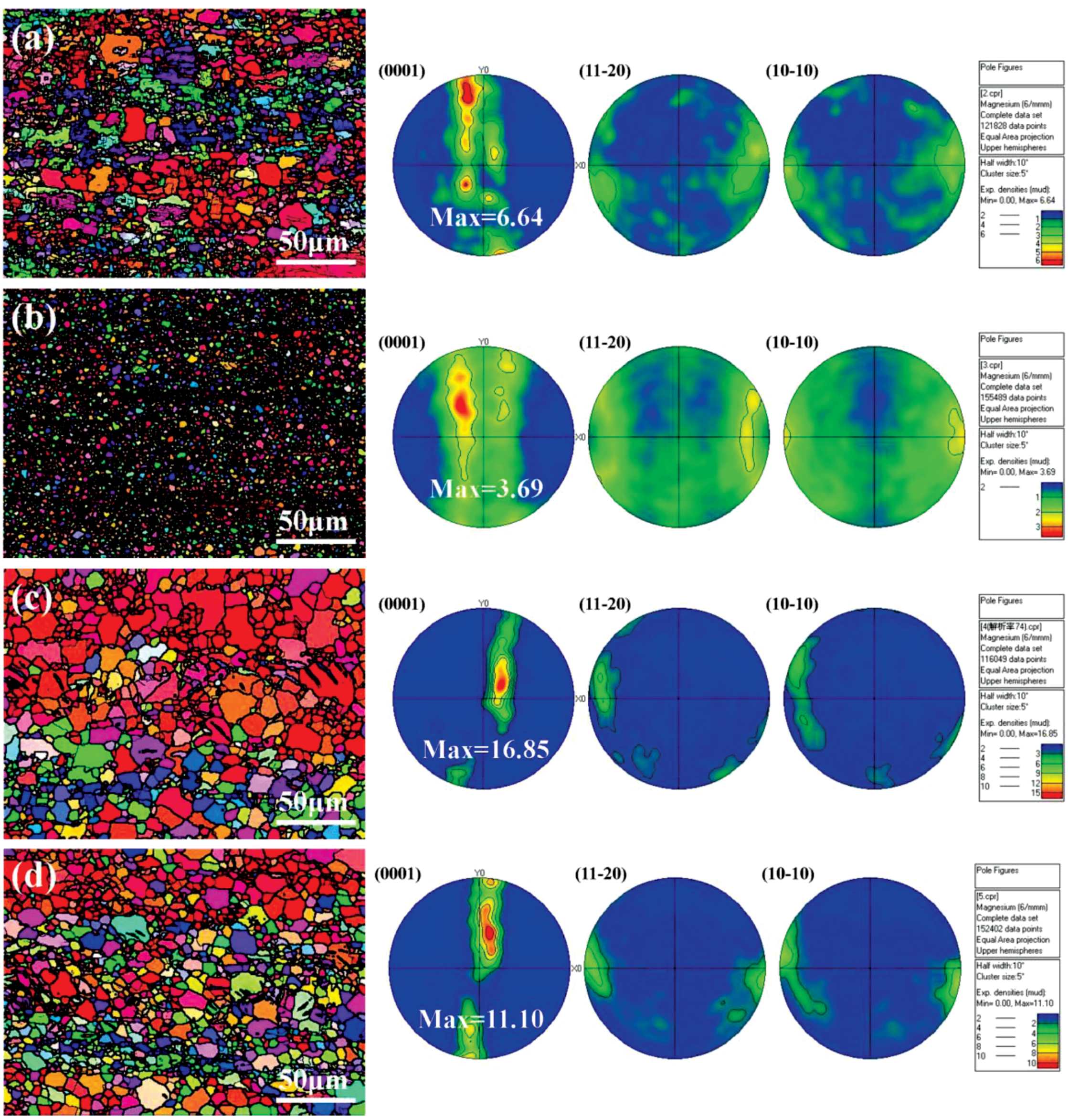


**Figure 5:** EBSD and pole figures of the four extruded alloys: a) TX31, b) TXK311, c) TXZ311, d) TXC311

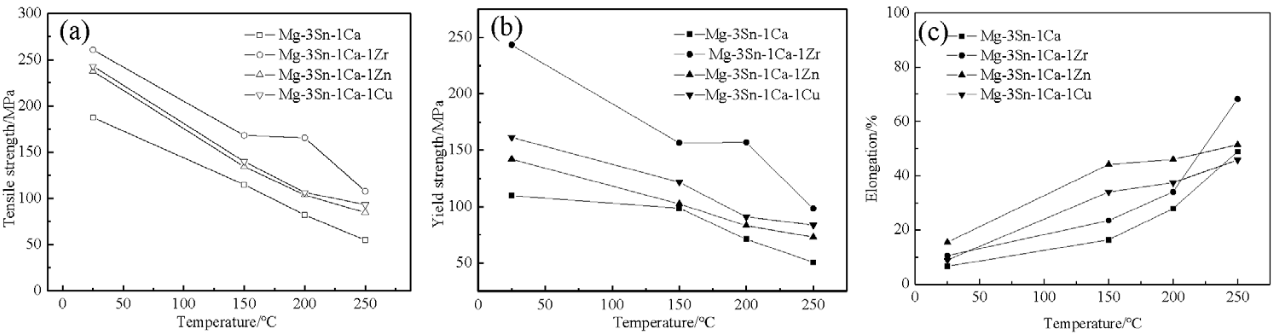


**Figure 6:** Mechanical properties of the four extruded alloys at room and high temperature

**Figure 5** shows pole figures of the four as-extruded alloys. It can be seen that the average grain sizes of TX31, TXK311, TXZ311 and TXC311 alloys are 3.5, 1.8, 5.1 and 4.5 μm, respectively. In an extruded alloy, added Zr can obviously refine the grains. However, the additions of Zn and Cu do not refine the grains. Moreover, it is found that the additions of Zn and Cu enhance the basal strength of the TX31 alloy, and the basal texture strength of the TXZ311 alloy is the highest, which is 16.85. On the contrary, when Zr is added to the TXZ311 and TXC311 alloys, the basal texture strength decreases significantly, being 3.69. The weakening of the basal deformation texture of magnesium alloys is beneficial for reducing anisotropy and improving the plastic deformation ability.

**Figure 6** shows the elevated-temperature mechanical properties of the four as-extruded alloys at 25–250 °C. It can be seen that the TXK311 alloy exhibits the highest

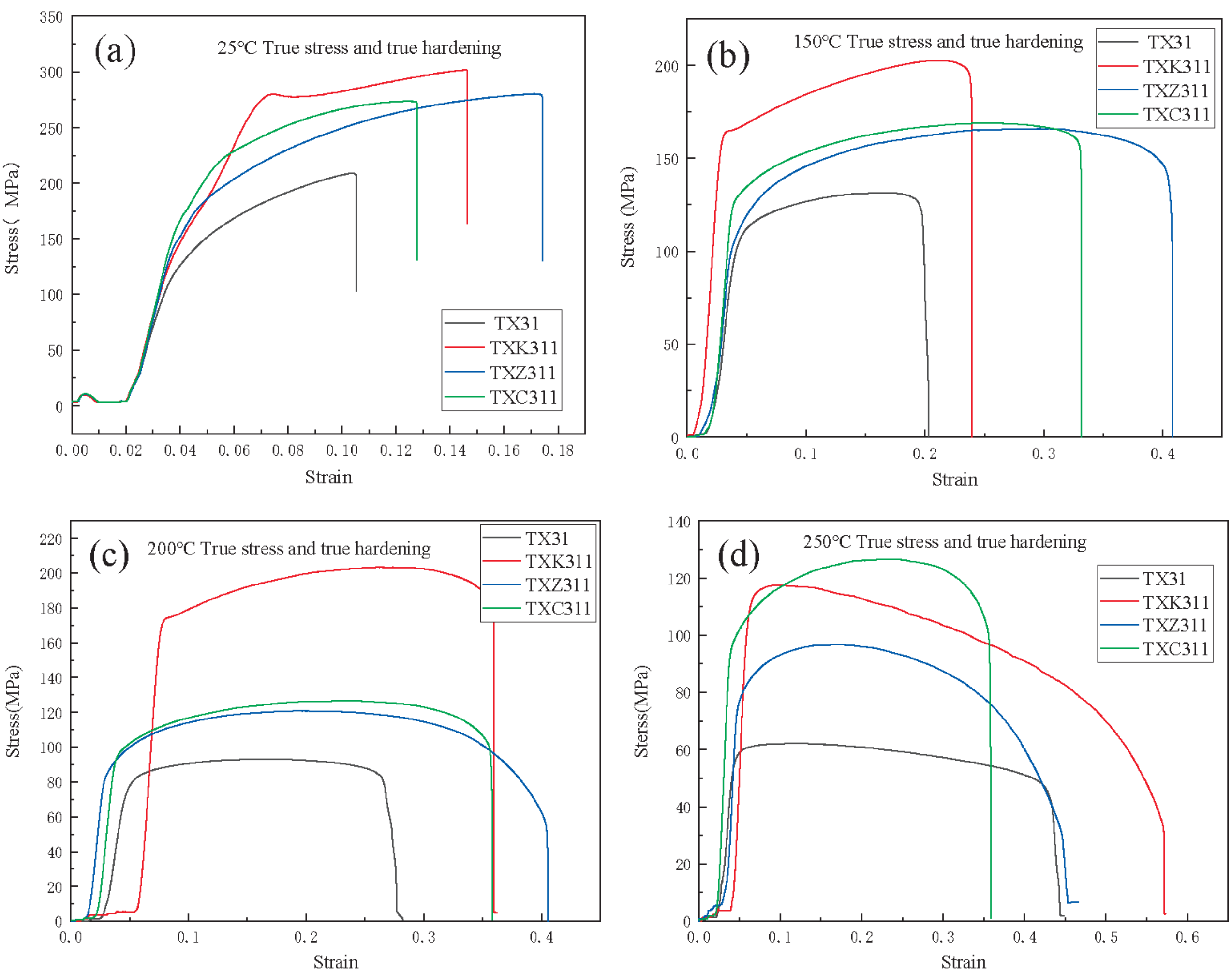


**Figure 7:** True tensile stress-strain curves of the as-extruded alloys at different temperatures: a) 25 °C, b) 150 °C, c) 200 °C, d) 250 °C

tensile strength and yield strength at temperatures of (25, 150, 200 and 250) °C, while TXZ311 exhibits the best plasticity at temperatures of (25, 150 and 200) °C, but TXK311 exhibits the best plasticity at 250 °C. At room temperature, the ultimate tensile strength (UTS) of TX31, TXK311, TXZ311 and TXC311 alloys is (187, 260, 237 and 243) MPa, respectively. The yield strength (YS) is (110, 243, 142 and 161) MPa, and the elongation (EL) is (6.7, 10.6, 15.5 and 8.9) %, respectively. From the results, it can be seen that the mechanical properties of the TX31 alloy were significantly improved by the Zr, Zn and Cu addition. When the temperature is elevated from 150 °C to 250 °C, the strength of the alloys except for the Mg-3Sn-1Ca-1Zr alloy decreases drastically, while the strength of the Mg-3Sn-1Ca-1Zr alloy exhibits little change between 150 °C and 200 °C. The maximum elongation of the TXK311 alloy can be 68.3 %, which is very beneficial for the next forming step of the alloy.

The representative true tensile stress-strain curves of the as-extruded samples at different temperatures are given in **Figure 7**. It can also be seen that the TXK311 alloy exhibits the best strength between 25 °C and 250 °C. However, an evident deterioration of the mechanical properties occurs in the Mg-3Sn-1Ca-1Cu alloy with the increase in the temperature.

**Figure 8** shows SEM images of the tensile fracture of the four as-extruded alloys at different temperatures. From the figure, it can be seen that there are ductile dimples and second-phase inclusions at the fracture surfaces of the four alloys under both room temperature and high temperature, indicating the presence of ductile fracture modes.[31,32] In **Figure 8a**, there are cleavage planes and tearing edges on the fracture surface of the TX31 alloy, indicating that the fracture of the alloy is mixed-mode fracture. After adding Zr, there are pores and a large number of equiaxed dimples on the fracture surface of the TXK311 alloy, and second-phase particles are found at the bottom of the dimples. The alloy exhibits ductile-fracture characteristics. After adding Zn, the alloy undergoes significant necking, with larger and deeper dimples, resulting in ductile fracture. Our analysis suggests that the larger particle size of the second phase in the TXZ31 alloy results in deeper and larger dimples. After adding Cu, there are pores and tearing edges on the fracture surface of the alloy, with deep dimples and ductile-fracture characteristics. According to the EDS re-

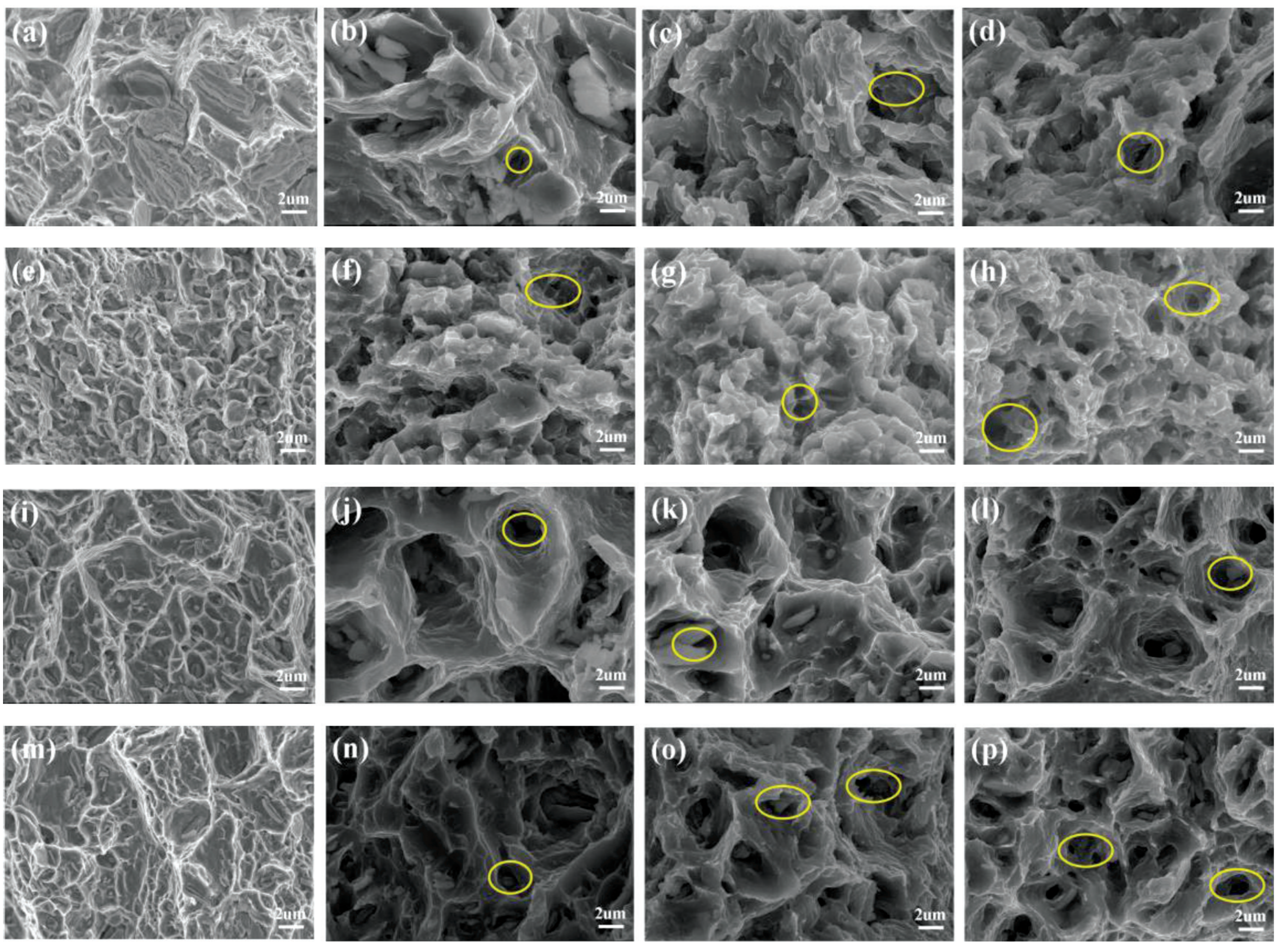


**Figure 8**: SEM images of samples' morphologies of tensile fracture of the as-extruded alloys at room and high temperatures: (a–d) TX31, (e–h) TXK311, (i–l) TXZ311, (m–p) TXC311, (a, e, i, m) 25 °C, (b, f, j, n) 150 °C, (c, g, k, o) 200 °C, (d, h, l, p) 250 °C

sults, the second-phase particles at the dimples of the TX31, TXK311 and TXZ311 alloys are determined to be the CaMgSn phase. The second-phase particles at the dimples of the TXC311 alloy are the CaMgSn phase and $Mg_2Cu$ phase. In addition, with the increase in the tensile temperature, there are micropores and more dimples at the fracture surface of the alloy. The dimples are larger and deeper, and the plasticity of the alloy is significantly improved.

Equiaxed dimples are microcracks formed at the interface between inclusions, second-phase particles and the matrix. The adjacent microcracks converge to produce microholes, causing a cavity growth and increment, and finally connecting to form fractures, leaving traces on the fracture surface. This indicates that the CaMgSn phase found in the dimples is the main reason for crack nucleation and propagation. TXK311 has a lot of fine dimples and CaMgSn phases, so its elongation can reach 68.3 % at 250 °C.

**Table 4:** Average grain sizes and maximum basal texture intensities of the four extruded samples

| Alloy | TX31 | TXK311 | TXZ311 | TXC311 |
|---|---|---|---|---|
| Grain size (μm) | 3.5 | 1.8 | 5.1 | 4.5 |
| Texture intensity | 6.64 | 3.69 | 16.85 | 11.1 |

In order to analyze the deformation mechanism of the samples, **Figure 9** plots the work-hardening rates derived from true stress versus true strain curves. The work-hardening behaviors of the four processed Mg alloys are obviously different. The initial rapid decrease in the work-hardening rate is due to the short period of elastoplastic transition. After the elastoplastic transition, the work-hardening rate starts to decrease slightly and both the grain size and texture intensity of the as-extruded samples exhibit great impacts on the work-hardening behaviors. Firstly, the strain-hardening rates of the four alloys can be shown as follows: TXK311> TXC311>TXZ311>TX31. When the strain is 0.09, the hardening ability of the TXK311 alloy decreases significantly. At this phase, the TX31, TXC311 and TXZ3111 alloys show a better strain-hardening ability. The TXK311 alloy exhibits a higher texture intensity compared with the TX31 and TXC311 alloys, as shown in **Table 4**. The higher texture intensity means a lower Schmid factor for the basal slip, promoting rapid hardening of the basal plane and a higher likelihood for cross-slipping onto the prismatic plane. Thus, higher decreasing speeds of the work-hardening rate occur in the TXK311 alloy (**Figure 9a**). **Figure 9b** shows changes in the strain-hardening indices of the four extruded alloys. It shows that the strain-hardening index of the TX31 alloy is the highest. However, as the yield strength of the alloy is low at this point, the strain-hardening indices of the other three alloys show little difference, indicating that there is little difference between the strain-hardening abilities of the TXK311, TXZ311 and TXC311 alloys. The poor strain rate of the TX31 alloy is due to a large number of CaMgSn hard brittle phases.

**Figure 10** shows the Schmidt factor plots of the four extruded alloys. It is worth noting that the critical shear stress (CRSS) required to activate basal slip largely depends on the Schmidt factor (SF) value of basal slip, which is related to the angle between the c-axis and the loading direction $\theta$.[33] Research has shown that the smaller the difference in the CRSS between the base and non-base surfaces, the easier it is to activate non-basal slip.[34] When Zr and Zn are added to an alloy, the basal slip SF increases significantly. Additionally, the difference in the SF along different directions decreases, which weakens the anisotropy of the alloy and ultimately leads to an increase in its ductility. In addition, the increase in the strength of the TXK311 alloy is due to the addition of Zr, which refines the grains and the second phase. Through fine-grain strengthening and second-phase dispersion strengthening, the yield strength of the TXK311 alloy is improved. In the TXZ311 alloy, the effect of solid-solution strengthening and precipitation

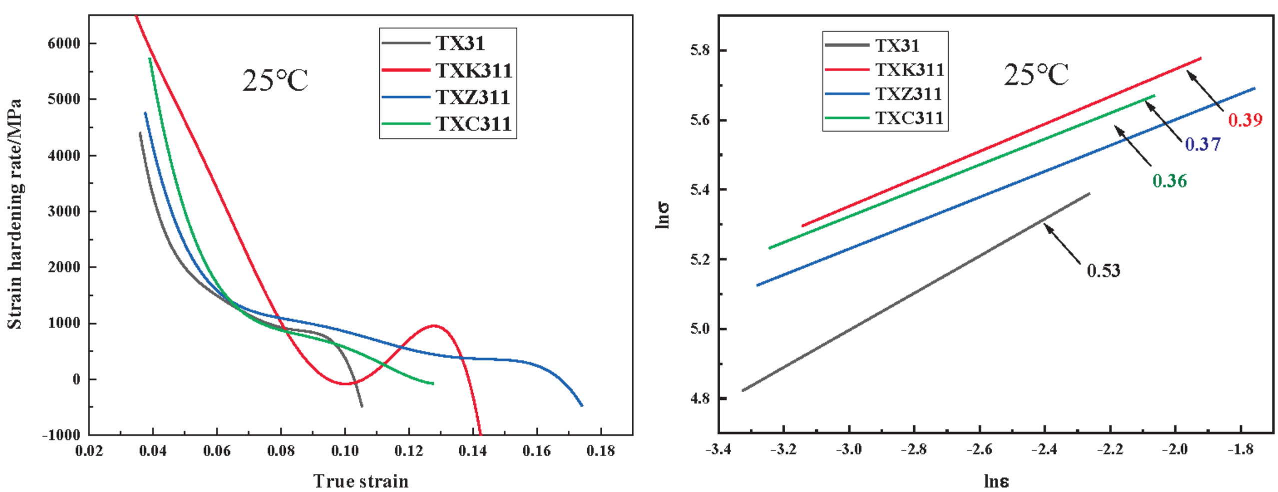


**Figure 9:** a) Strain-hardening rates and b) strain-hardening indices of the four extruded alloys

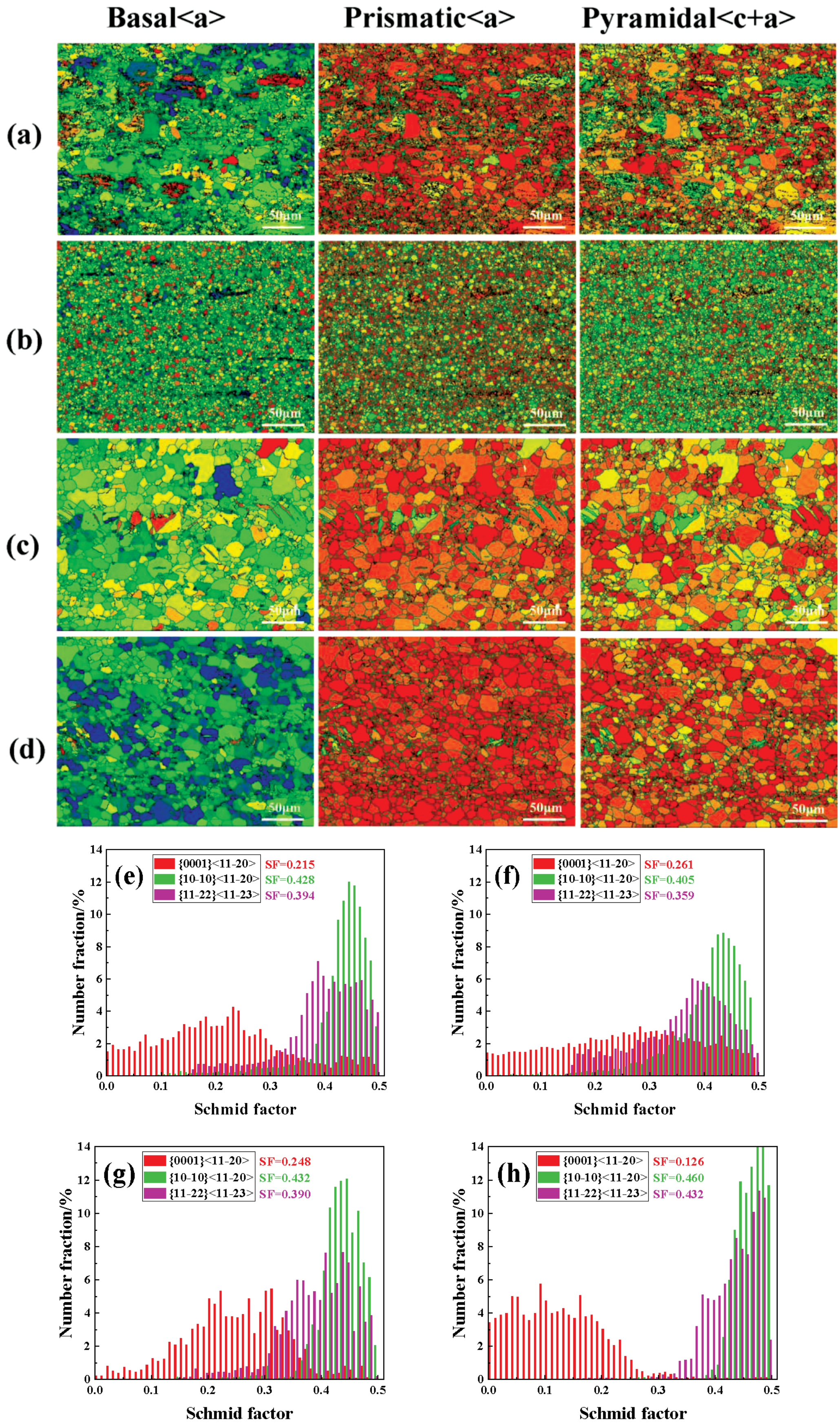


**Figure 10:** Distribution of Schmid factors: (a, e) TX31; (b, f) TXK311; (c, g) TXZ311; (d, h) TXC311

strengthening of Zn reduces the difference between the substrate slip and non-substrate slip, reduces anisotropy, and increases the strength and plasticity. When Cu is added to the alloy, it forms a spherical $Mg_2Cu$ phase due to the low solid solubility of Cu in magnesium (0.55 %). The TXC311 alloy's strength is enhanced by solid-solution strengthening and second-phase strengthening. However, the anisotropy of basal slip and non-basal slip is significantly increased, which results in a relatively lower plasticity compared to that of the TXZ311 alloy. When Zr is added to TX31, a CaMgSn phase and fine grains are produced in the alloy. These serve as a second phase and lead to fine-grain strengthening, resulting in TXK311 having the most desirable mechanical properties.

## 4 CONCLUSIONS

In this study, the effects of Zr, Zn and Cu on the high-temperature mechanical properties of an extruded Mg-3Sn-1Ca alloy were studied, and the following conclusions were drawn:

The microstructure of the TX31 alloy is determined by the $\alpha$-Mg phase and CaMgSn phase. With an addition of Zr, the grain size decreases, the strength of the basal texture weakens and no new second phase is formed. After an addition of Zn, it solidly dissolves in the magnesium matrix, without forming a second phase containing Zn. A small amount of $Mg_2Sn$ phase precipitates in the alloy, and the grain size of the alloy increases. An addition of Cu increases the grain size and causes the formation of a spherical $Mg_2Cu$ phase, resulting in an increase in the strength of the basal texture.

Among the four extruded alloys, the Mg-3Sn-1Ca-1Zr alloy exhibits the best mechanical properties at temperatures of (25, 150, 200 and 250) °C. The high strength of the Mg-3Sn-1Ca-1Zr alloy is attributed to its smaller grain size (1.8 μm), which plays a role in fine-grain strengthening. The high plasticity at 250 °C is attributed to the weak texture strength (3.69) of the Mg-3Sn-1Ca-1Zr alloy, which reduces anisotropy and improves the plastic-deformation ability, so it is very beneficial for the next forming step.

### Acknowledgements

The authors acknowledge the financial support from the Key Project of the Education Department of the Liaoning Province [LJKZ1171], China Postdoctoral Fund [2020M680978], Liaoning Province Doctoral Start-Up Fund Project [2020-BS-260], Natural Science Foundation of the Fujian Province [2021J05232] and Science and Technology Planning Project of Longyan [2021LYF9012].

## 5 REFERENCES

[1] S. V. S. Prasad, S. B. Prasad, K. Verma, R. K. Mishra, V. Kumar, S. Singh, The role and significance of Magnesium in modern day research – A review, Journal of Magnesium and Alloys, 10 (**2022**) 1,1–61, doi:10.1016/j.jma.2021.05.012

[2] S. Lesz, B. Hrapkowicz, M. Karolus, K. Gołombek, Characteristics of the Mg-Zn-Ca-Gd Alloy after Mechanical Alloying, Materials, 14 (**2021**) 1, 226, doi:10.3390/ma14010226

[3] D. Dvorský, J. Kubásek, D. Vojtech, M. Čavojský, P. Minárik, Effect of heat pre-treatment and extrusion on the structure and mechanical properties of WZ21 magnesium alloy, Materials and Technology, 52 (**2018**) 4, 499–505, doi:10.17222/mit.2017.214

[4] W. L. Wang, Y. L. Qiu, J. D. Jia, X. Yan, W. Zhang, Influence of samarium on the microstructure and mechanical properties of Mg-Y-Zn-Zr alloys, Mater. Tehnol., 52 (**2018**) 4, 405–410, doi:10.17222/mit.2017.175

[5] C. C. Xiang, Z. D. Xiao, H. L. Ding, Z. J. Wang, Compressive Properties and Energy Absorption Characteristics of Extruded Mg-Al-Ca-Mn Alloy at Various High Strain Rates, Materials (Basel, Switzerland), 14 (**2020**) 1, doi:10.3390/ma14010087

[6] D. Dvorsky, J. Kubasek, D. Vojtech, P. Minárik, J. Stráská, The effect of Y, Gd and Ca on the ignition temperature of extruded magnesium alloys, Materials and Technology, 54 (**2020**) 5,669–675, doi:10.17222/mit.2019.284

[7] P. L. Jiang, C. Blawert, J. Bohlen, M. L. Zheludkevich, Corrosion performance, corrosion fatigue behavior and mechanical integrity of an extruded Mg-4Zn-0.2Sn alloy, Journal of Materials Science & Technology, 59 (**2020**),107–116, doi:10.1016/j.jmst.2020.04.042

[8] H. M. Liu, Y. G. Chen, Y. B. Tang, S. H. Wei, G. Niu, The microstructure, tensile properties, and creep behavior of as-cast Mg-(1-10) % Sn alloys, Journal of Alloys and Compounds, 440 (**2007**) 1–2, 122–126, doi:10.1016/j.jallcom.2006.09.024

[9] H. C. Pan, G. W. Qin, M. Xu, H. Fu, Y. P. Ren, F. S. Sheng, Z. Y. Gao, C. Y. Zhao, Q. S. Yang, J. She, B. Song, Enhancing mechanical properties of Mg-Sn alloys by combining additions of Ca and Zn, Materials & Design, 83 (**2015**),736–44, doi:10.1016/j.matdes.2015.06.032

[10] A. Baghani, H. Khalilpour, S. M. Miresmaeili, Microstructural evolution and creep properties of Mg-4Sn alloys by addition of calcium up to 4 wt.%, Transactions of Nonferrous Metals Society of China, 30 (**2020**) 4, 896–904, doi:10.1016/S1003-6326(20)65263-3

[11] K. P. Rao, Y. V. R. K. Prasad, N. Hort, K. U. Kainer, Hot workability characteristics of cast and homogenized Mg-3Sn-1Ca alloy, Journal of Materials Processing Technology, 201 (**2008**) 1–3, 359–363, doi:10.1016/j.jmatprotec.2007.11.148

[12] M. Kavyani, G. R. Ebrahimi, H. R. Ezatpour, M. Jahazi, Microstructure refinement, mechanical and biocorrosion properties of Mg-Zn-Ca-Mn alloy improved by a new severe plastic deformation process, Journal of Magnesium and Alloys, 10 (**2022**) 6, 1640–1662, doi:10.1016/j.jma.2020.11.013

[13] F. Wang, Y. Feng, M. S. Li, X. Y. Teng, Effect of Ca and Zr additions and aging treatments on microstructure and mechanical properties of Mg-Sn alloy, Materials Science Forum, Trans Tech Publications Ltd, 993 (**2020**), 152–160, doi:10.4028/www.scientific.net/MSF.993.152

[14] C. M. Wang, L. M. Zeng, W. L. Zhang, F. Q. Tang, W. C. Ding, S. F. Xiao, T. X. Liang, Enhanced mechanical properties and corrosion resistance of rolled Mg-1.5Sn-0.5Ca alloy by Ce microalloying, Materials Characterization, 179 (**2021**), 111325, doi:10.1016/j.matchar.2021.111325

[15] Z. R. Zeng, M. Z. Bian, S. W. Xu, C. H. J. Davies, N. Birbilis, J. F. Nie, Effects of dilute additions of Zn and Ca on ductility of magnesium alloy sheet, Materials Science and Engineering: A, 674 (**2016**), 459–471, doi:10.1016/j.msea.2016.07.049

[16] L. Y. Wei, J. Y. Li, Y. Zhang, H. Y. Lai, Effects of Zn content on microstructure, mechanical and degradation behaviors of Mg-xZn-0.2 Ca-0.1 Mn alloys, Materials Chemistry and Physics, 241 (**2020**), 122441. doi:10.1016/j.matchemphys.2019.122441

[17] Q. H. Wang, H. W. Zhai, L. T. Liu, Z. Y. Jin, L. Y. Zhao, J. J. He, J. Bin, Exploiting an as-extruded fine-grained Mg-Bi-Mn alloy with strength-ductility synergy via dilute Zn addition, Journal of Alloys and Compounds, 924 (**2022**), 166337. doi:10.1016/j.jallcom.2022.166337

[18] H. Y. Wang, J. Rong, G. J. Liu, M. Zha, C. Wang, D. Luo, Q. C. Jiang, Effects of Zn on the microstructure and tensile properties of as-extruded Mg-8Al-2Sn alloy, Materials Science and Engineering: A, 698 (**2017**), 249–255, doi:10.1016/j.msea.2017.05.055

[19] W. N. Tang, S. S. Park, B. S. You, Effect of the Zn content on the microstructure and mechanical properties of indirect-extruded Mg-5Sn-xZn alloys, Materials & Design, 32 (**2011**) 6, 3537–3543, doi:10.1016/j.matdes.2011.02.012

[20] S. Dai, F. Wang, Z. Wang, Z. Liu, P. L. Mao, Effect of Cu on microstructure, mechanical properties, and texture evolution of ZK60 alloy fabricated by hot extrusion-shearing process, Transactions of Nonferrous Metals Society of China, 30 (**2020**) 6, 1511–1523, doi:10.1016/S1003-6326(20)65315-8

[21] Y. Q. Tang, Y. G. Chen, S. F. Xiao, W. C. Ding, C. M. Wang, X. Liu, Microstructure, Mechanical Properties and Compressive Creep Behavior of as-Cast Mg-5Sn-(0≈2) Cu Alloys, Rare Metal Materials and Engineering, 43 (**2014**) 6, 1291–1295, doi:10.1016/S1875-5372(14)60109-0

[22] X. Li, J. W. Liu, C. P. Luo, Precipitation behavior of cast ZC62 magnesium alloy, Acta Metallurgica Sinica, 42 (**2006**), 733–738, doi:10.3321/j.issn:0412-1961.2006.07.011

[23] H. M. Zhu, G. Sha, J. W. Liu, C. L. Wu, C. P. Luo, Z. W. Liu, R. K. Zheng, S. P. Ringer, Microstructure and mechanical properties of Mg-6Zn-xCu-0.6Zr (wt.%) alloys, Journal of Alloys and Compounds, 509 (**2011**), 3526–3531, doi:10.1016/j.jallcom.2010.12.165

[24] C. Wang, T. J. Luo, Y. T. Liu, T. Lin, Y. S. Yang, Microstructure and mechanical properties of Mg-5Zn-3.5 Sn-1Mn-0.5 Ca-0.5 Cu alloy, Materials Characterization, 147 (**2019**), 406–413, doi:10.1016/j.matchar.2018.11.029

[25] T. Homma, C. L. Mendis, K. Hono, S. Kamado, Effect of Zr addition on the mechanical properties of as-extruded Mg-Zn-Ca-Zr alloys, Materials Science and Engineering: A, 527 (**2010**) 9, 2356–2362, doi:10.1016/j.msea.2009.12.024

[26] F. J. Xing, F. Guo, J. Su, X. P. Zhao, H. X. Cai, The existing forms of Zr in Mg-Zn-Zr magnesium alloys and its grain refinement mechanism, Materials Research Express, 8 (**2021**) 6, 066516, doi:10.1088/2053-1591/ac083c

[27] C. Xu, T. Nakata, G. H. Fan, X. W. Li, G. Z. Tang, L. Geng, S. Kamado, Microstructure and mechanical properties of extruded Mg-Gd-Y-Zn alloy with Mn or Zr addition, Journal of Materials Science, 54 (**2019**), 10473–10488, doi:10.1007/s10853-019-03607-4

[28] F. Kiani, J. X. Lin, A. Vahid, K. Munir, C. Wen, Y. C. Li, Mechanical and corrosion properties of extruded Mg-Zr-Sr alloys for biodegradable implant applications, Materials Science and Engineering: A, 831 (**2022**), 142192, doi:10.1016/j.msea.2021.142192

[29] C. M. Wang, S. Guo, L. M. Zeng, D. S. Zheng, J. C. Xu, M. N. Yang, T. X. Liang, Effects of second phases on microstructure, microhardness, and corrosion behavior of Mg-3Sn-(1Ca) alloys, Materials, 12 (**2019**) 16, 2515, doi:10.3390/ma12162515

[30] H. C. Pan, H. Fu, Y. P. Ren, Q.Y. Huang, Z. Y. Gao, J. She, G. W. Qin, Q. S. Yang, B. Song, F. S. Pan, Effect of Cu/Zn on microstructure and mechanical properties of extruded Mg-Sn alloys, Materials Science and Technology, 32 (**2016**) 12, 1240–1248, doi:10.1080/02670836.2015.1115604

[31] Y. Z. Meng, J. M. Yu, K. Liu, H. S. Yu, F. Zhang, Y. J. Wan, Z. M. Zhang, N. Luo, H. H. Wang, The evolution of long-period stacking ordered phase and its effect on dynamic recrystallization in Mg-Gd-Y-Zn-Zr alloy processed by repetitive upsetting-extrusion, Journal of Alloys and Compounds, 828 (**2020**), 154454, doi:10.1016/j.jallcom.2020.154454

[32] W. J. Wu, W. Z. Chen, L. X. Zhang, X. M. Chen, H. X. Wang, W. K. Wang, W. C. Zhang, Improvement of tension/compression asymmetry for high-performance ZK61 magnesium alloy rod via tailoring deformation parameters: Upsetting-extrusion temperature and upsetting ratio, Materials Science and Engineering: A, 823 (**2021**), 141767, doi:10.1016/j.msea.2021.141767

[33] S. H. Kim, S. H. Park, Underlying mechanisms of drastic reduction in yield asymmetry of extruded Mg-Sn-Zn alloy by Al addition, Materials Science and Engineering: A, 733 (**2018**), 285–290, doi:10.1016/j.msea.2018.07.063

[34] Q. H. Wang, B. Jiang, A. Tang, S. X. Ma, Z. T. Jiang, Y. F. Chai, B. Luo, F. S. Pan, Ameliorating the mechanical properties of magnesium alloy: Role of texture, Materials Science and Engineering: A, 689 (**2017**), 395–403, doi:10.1016/j.msea.2017.02.067